Changes in wind speed under heat waves enhance urban heat islands in the Beijing Metropolitan Area

Article

Published Version

Changes in Wind Speed under Heat Waves Enhance Urban Heat Islands in the Beijing Metropolitan Area

DAN LI

Department of Earth and Environment, Boston University, Boston, Massachusetts

TING SUN

State Key Laboratory of Hydro-Science and Engineering, Department of Hydraulic Engineering, Tsinghua University, Beijing, China

MAOFENG LIU

Department of Civil and Environmental Engineering, Princeton University, Princeton, New Jersey

LINLIN WANG AND ZHIQIU GAO

State Key Laboratory of Atmospheric Boundary Layer Physics and Atmospheric Chemistry, Institute of Atmospheric Physics, Chinese Academy of Sciences, Beijing, China

(Manuscript received 3 March 2016, in final form 3 July 2016)

ABSTRACT

The interaction between urban heat islands (UHIs) and heat waves (HWs) is studied using measurements collected at two towers in the Beijing, China, metropolitan area and an analytical model. Measurements show that 1) the positive interaction between UHIs and HWs not only exists at the surface but also persists to higher levels (up to ~70 m) and 2) the urban wind speed is enhanced by HWs during daytime but reduced during nighttime as compared with its rural counterpart. A steady-state advection–diffusion model coupled to the surface energy balance equation is then employed to understand the implication of changes in wind speed on UHIs, which reveals that the observed changes in wind speed positively contribute to the interaction between UHIs and HWs in both daytime and nighttime. The vertical structure of the positive interaction between UHIs and HWs is thus likely an outcome resulting from a combination of changes in the surface energy balance and wind profile.

1. Introduction

Heat waves (HWs) are prolonged periods of high temperatures and they are among the deadliest natural disasters (Anderson and Bell 2009, 2011; D'Ippoliti et al. 2010; Kovats and Hajat 2008; Petkova et al. 2014). Cities are arguably more vulnerable to HWs than rural areas because of the background urban heat island (UHI) effect; that is, cities are typically hotter than rural areas even under non-HW conditions (Arnfield 2003; Grimmond 2007; Oke 1982). An important question that needs to be answered is whether the UHI effect will be enhanced by HWs. If UHIs were enhanced by HWs (i.e., there is a positive or synergistic interaction between UHIs and HWs), city residents would face higher health risks than a simple addition of the risks associated with HWs and the background UHIs. This is particularly relevant within the context of global climate change since studies have shown that the frequency and duration of HWs are very likely to be increased under a warming climate (IPCC 2013; Lau and Nath 2014; Mishra et al. 2015; Peterson et al. 2013; Smith et al. 2013).

A few recent studies have attempted to answer this question from theoretical, numerical, and experimental perspectives. Li and Bou-Zeid (2013, hereinafter LBZ13) examined observational data from ground weather stations and found that the daytime UHI effect over the Baltimore–Washington area in the United

Corresponding author address: Dan Li, Department of Earth and Environment, Boston University, 685 Commonwealth Ave., Boston, MA 02215.
E-mail: lidan@bu.edu

DOI: 10.1175/JAMC-D-16-0102.1

States was enhanced during an HW episode. They also conducted urban climate simulations using the newly developed Princeton Urban Canopy Model coupled into the Weather Research and Forecasting Model (Li and Bou-Zeid 2014; Li et al. 2014), which showed that the UHI effect defined based on the near-surface air temperature was enhanced during the HW period, while the UHI effect defined based on the surface temperature was enhanced in the post-HW period. Furthermore, they developed a steady-state analytical model based on the solution to the advection–diffusion equations for water vapor and heat coupled to the surface energy balance equation and found that the UHI effect was mostly controlled by the urban–rural contrast of water availability. Hence changing the partition of available energy into sensible heat flux and latent heat flux is very effective in altering the UHI effect. Li et al. (2015, hereinafter L15) closely followed the study of LBZ13 but focused on observed changes in the surface energy balance under HWs. Using datasets collected at two flux towers (one located at an urban site and the other located at a rural site in the Beijing metropolitan area), they found that HWs enhance sensible heat flux and reduce latent heat flux at the urban site relative to the rural site, which is key to explaining the enhanced UHI effect during daytime. In addition, cities store more heat during daytime under HWs, which is later released and enhances the UHI effect during nighttime. These observational findings are consistent with the numerical and analytical model results in LBZ13.

These two previous studies have primarily focused on the near-surface and surface UHIs and largely neglected the role of changes in the wind speed, although it was alluded to by the analytical model of LBZ13 that changes in the wind speed may contribute to or negate the positive interaction between UHIs and HWs. This motivates us to address the following two remaining questions in this paper: first, is the positive interaction between UHIs and HWs persistent in the vertical direction? Second, what is the role of changes in wind speed in modulating the interaction between UHIs and HWs? To address these questions, field measurements collected in the Beijing metropolitan area in China, which have been studied in L15, and the model of LBZ13 are used.

2. Data and methodology

a. Observational data

Observational data collected at two flux towers, one located in the city of Beijing (39.97°N, 116.37°E) and the other located in a rural place adjacent to Beijing called Xianghe (39.78°N, 116.95°E), were used in this study. More details about the data can be found in Wang et al. (2014, 2015) and L15. The 325-m-tall Beijing tower includes hourly air temperature, relative humidity, wind speed, and wind direction measurements at 15 levels above the ground, as shown in Yu et al. (2013). In this study, data at the lowest seven levels (i.e., 8, 15, 32, 47, 63, 80, and 102 m) are used. It also includes turbulence measurements at three levels (i.e., 47, 140, and 280 m) from which 30-min sensible and latent heat fluxes are calculated following Li and Bou-Zeid (2011), Li et al. (2012), and Wang et al. (2014). The Xianghe flux tower also includes hourly air temperature, relative humidity wind speed, and wind direction at seven levels above the ground (i.e., 8, 16, 32, 48, 63, 80, and 100 m), which correspond to the lowest seven levels at the Beijing flux tower. It also includes turbulence measurements at two levels (32 and 64 m).

HW periods in the summer (June, July, and August) of 2009 and 2010 are identified using the method in Meehl and Tebaldi (2004) and have been presented in L15. Observations during the 44 HW days are averaged to present the ''heatwave'' conditions and those during the 140 non-HW days are averaged to present the ''background'' conditions. We stress that it is not our goal to study the large-scale circulation patterns associated with HWs (Lau and Nath 2012, 2014). Rather, our focus is on the local responses of urban and rural surfaces and boundary layers to HWs, and hence we will only present observational data collected at the two flux towers. We also note that there are other definitions for HW (Robinson 2001; Smith et al. 2013) and exploring the differences among various HW definitions is outside our scope.

b. An analytical model

To facilitate our understanding of the impact of changes in wind speed on the synergistic interactions between UHIs and HWs, the analytical model of LBZ13 is employed here, which was inspired by previous studies solving the advection–diffusion equations for water vapor and heat coupled to the surface energy balance equation over a lake surface surrounded by land (Yeh and Brutsaert 1971a,b). The advection–diffusion equations for water vapor and heat are used here because we are primarily interested in the flow and transport across the urban–rural gradient (i.e., at regional scales) rather than within the urban canopy (i.e., at neighborhood scales). The validity of using advection–diffusion equations to study internal boundary layer development has been reviewed elsewhere (Garratt 1990), and the neglect of horizontal diffusion has been justified using numerical simulations (Yeh and Brutsaert 1971a). The

model produces results that are qualitatively consistent with observational data, which has been discussed in L15.

In essence, the model solves the advection–diffusion equations for water vapor and heat with prescribed vertical wind and turbulent diffusivity profiles. The surface boundary conditions are represented by the surface energy balance equation and an equation describing the availability of soil water for evapotranspiration. As a result, the major factors influencing the UHI effect—such as the urban–rural contrasts of soil water, albedo, and heat admittance—are captured by the model directly or indirectly. Full details about the derivation of this model can be found in the study of LBZ13, which also showed the sensitivity of UHI to different factors. In this study, only the final expression of the model for the UHI effect is shown and we will primarily focus on the sensitivity of UHI to changes in the wind speed:

$$\mathrm{UHI}(x,z) = \left(1 - \frac{\beta_u}{\beta_r}\right) T_{\mathrm{rs}}^{*} f_1(x,z) + g(u)\Delta Q f_2(x,z), \quad (1)$$

where x is the longitudinal direction and z is the vertical direction. Here UHI (x, z) is the difference between the urban air temperature at x and z and its rural counterpart at z (note the rural area is assumed to be infinitely long, and thus the rural air temperature is only a function of z). The ratio β is the actual specific humidity divided by the saturated specific humidity at the surface, and hence β ranges from 0 to 1 with 0 indicating a completely dry surface and 1 indicating a saturated surface (LBZ13). The subscripts u and r indicate urban and rural, respectively, and thus β_u/β_r indicates the urban–rural contrast of surface wetness, which is mainly caused by the urban–rural contrast of soil water. The term T_{rs}^{*} is a characteristic temperature scale representing the sensitivity of UHI to the urban–rural moisture availability difference, and ΔQ is the difference in available energy, which is defined as the sum of sensible heat flux H and latent heat flux LE urban and rural areas; ΔQ can be caused by urban–rural contrasts of albedo, heat admittance, anthropogenic heat flux, and other factors. Here $g(u)$ is a positive, monotonic function that decreases with the wind speed u (LBZ13). From Eq. (1) it is clear that the sensitivity of UHI to changes in the wind speed u is modulated by ΔQ, which can be either positive or negative. As shall be seen later, positive ΔQ tends to occur during nighttime and negative ΔQ tends to occur during daytime. When ΔQ is positive, the UHI effect increases with decreasing u; when ΔQ is negative, the UHI effect increases with increasing u. The expressions g, f_1, and f_2 can be found in LBZ13.

3. Results

Figure 1 shows the averaged vertical profiles of air temperature under HW and non-HW (or background) conditions for daytime (Fig. 1a) and nighttime (Fig. 1b). As can be seen, urban temperatures are always higher than rural temperatures, implying positive UHIs in the lower atmosphere. Both urban and rural temperatures are enhanced under HW conditions. Nighttime rural temperatures increase with height, which is consistent with the temperature profile in a typical nocturnal boundary layer; however, nighttime urban temperatures are almost uniform with height, suggesting stronger mixing in urban areas possibly due to larger anthropogenic heat fluxes.

The UHIs are also calculated and presented. Under background conditions (Fig. 1c), the daytime UHIs remain all positive below 100 m while the nighttime UHIs become increasingly smaller as the height increases and become almost zero at about 100 m. This suggests that the daytime urban boundary layer is much higher than the nighttime counterpart. It is clear that UHIs are enhanced under HW conditions, suggesting positive or synergistic interactions between HWs and UHIs as observed in previous studies (LBZ13; L15). These synergistic interactions are stronger during nighttime than during daytime, which is also consistent with the results in LBZ13 and L15. However, what is not observed before is that these synergistic interactions prevail in the vertical direction up to about 70 m and become smaller at higher levels. As shall be seen later, changes in the vertical wind profile, in addition to changes in the surface energy budget, also strongly contribute to the synergistic interactions between HWs and UHIs.

To understand the role of wind speed (WS) changes in modulating the synergistic interactions between UHIs and HWs, Fig. 2 examines the urban–rural wind speed differences, which are mostly negative. This is with the fact that momentum roughness length over urban areas is generally larger. Interestingly, daytime changes (Fig. 2a) are different from their nighttime counterparts (Fig. 2b). Using the rural as a reference, HWs enhance (reduce) the urban wind speed during daytime (nighttime). The changes in terms of magnitude are on the order of 0.1–0.5 m s^{-1}. The daytime wind speed differences are more uniform in the vertical direction when it is above 30 m probably because of the stronger mixing during daytime.

It can be seen from the analytical model [Eq. (1)] that the sensitivity of UHI to wind speed strongly depends on the sign of urban–rural available energy difference (ΔQ). Therefore, the measured urban–rural available energy difference is compared in Fig. 3. Since turbulent

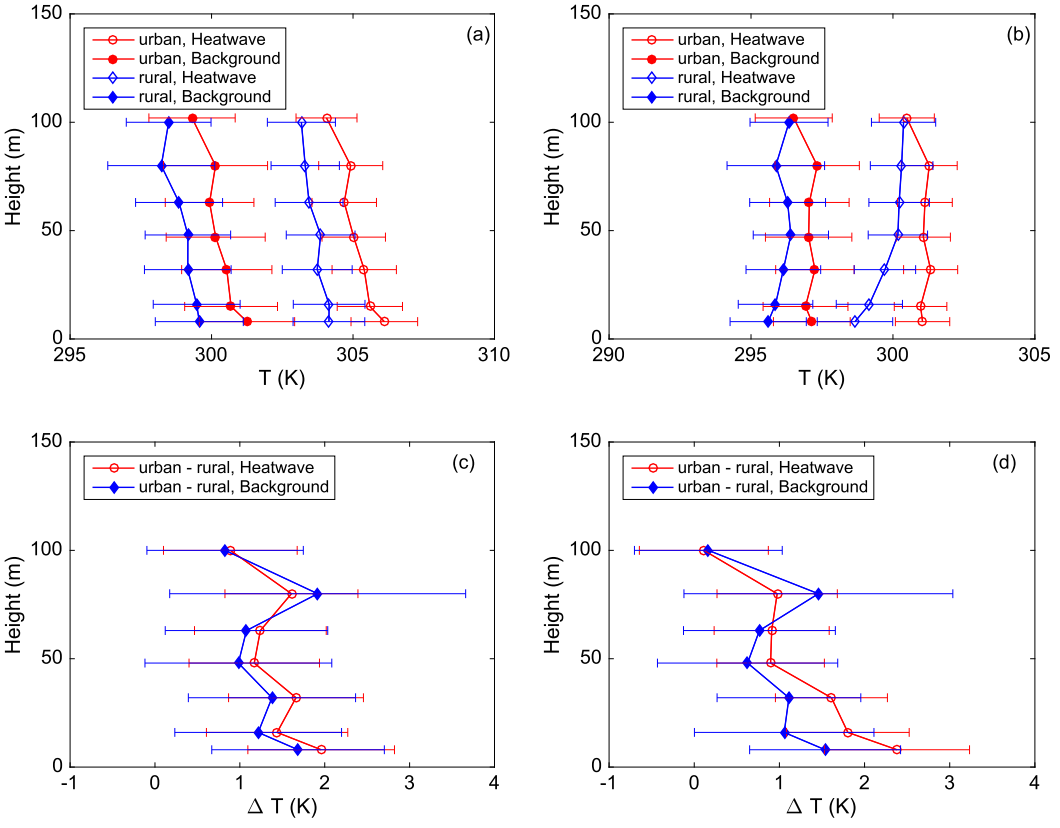

FIG. 1. The averaged vertical profiles of air temperatures under (a) daytime and (b) nighttime conditions. (c),(d) The differences between urban and rural temperatures, namely, the UHIs. Error bars denote 1 std dev.

fluxes are measured at multiple levels, two methods of calculating ΔQ are used: in Fig. 3a, the averages of fluxes measured at multiple levels (47, 140, and 280 m for the urban site; 32 and 64 m for the rural site) are used while in Fig. 3b, the fluxes measured at a single level (140 m for the urban site and 32 m for the rural site) are used. Previous studies have shown that 47 m in the urban area is still within the roughness sublayer (Miao et al. 2012) so fluxes at 140 m are used to represent the urban condition in Fig. 3b. It is clear that the urban–rural available

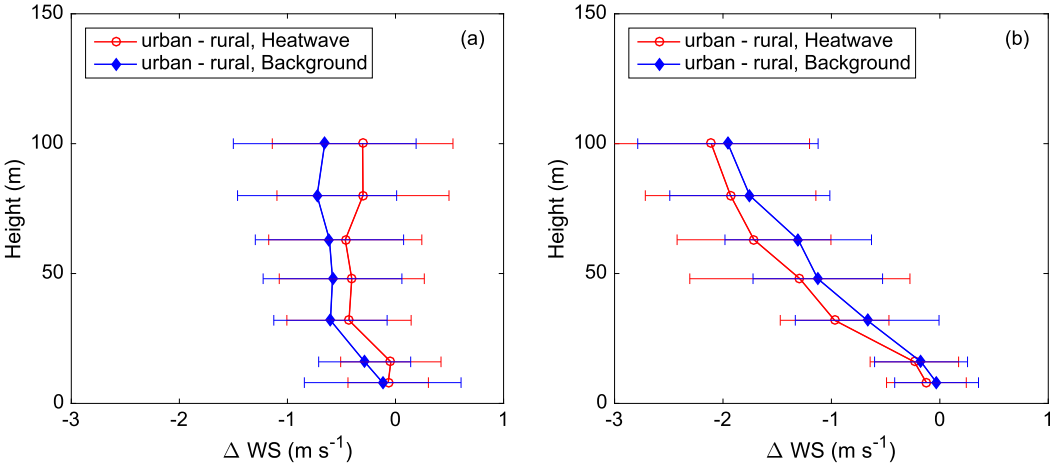

FIG. 2. The averaged vertical profiles of urban–rural WS differences under (a) daytime and (b) nighttime conditions. Error bars denote 1 std dev.

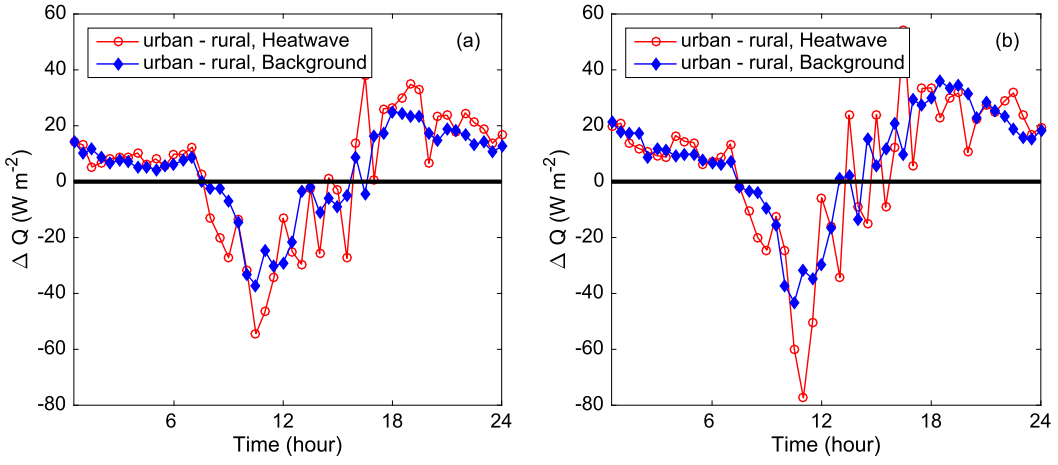

FIG. 3. (a),(b) The averaged diurnal cycles of urban–rural available energy Q differences under HW and background conditions. Local standard time is used here. To calculate $Q = H + LE$, (a) uses the averages of fluxes measured at three levels (i.e., 47, 140, and 280 m) in the urban area and the averages of fluxes measured at two levels (i.e., 32 and 64 m) in the rural area; (b) uses the fluxes measured at 140 m in the urban area and the fluxes measured at 32 m in the rural area.

energy differences from both methods are primarily positive during nighttime but negative during daytime. This is due to the fact that rural areas have a much larger latent heat flux during daytime, while urban areas have a larger sensible heat flux during nighttime when latent heat fluxes of both urban and rural areas are nearly zero.

As a result of positive (negative) ΔQ during nighttime (daytime), the sensitivity of UHI to changes in wind speed in the daytime differs from that in the nighttime. As an illustration, Fig. 4 shows the simulated UHI effect using Eq. (1) as a function of wind speed with typical daytime ($\Delta Q = -20\,\mathrm{W\,m^{-2}}$) and nighttime ($\Delta Q = 20\,\mathrm{W\,m^{-2}}$) values. Two cases that have different β_u/β_r values are shown to emphasize that the UHI effect is also very sensitive to the water availability difference, as pointed out by the study of LBZ13. Figure 4 clearly shows that the daytime UHI effect is enhanced as wind speed *increases* while the nighttime UHI effect is enhanced as wind speed *decreases*. Close inspection of temperature profiles (not shown here) reveals that during daytime ($\Delta Q < 0$), increasing wind speed enhances the sensible heat flux in urban areas, whose heating effect on the urban atmosphere is stronger than the also enhanced advective cooling effect (i.e., cooler air from rural areas is brought to urban areas); however, during nighttime, increasing wind speed enhances the advective cooling effect more significantly than the surface heating effect and hence results in a reduction in UHIs. Combining Figs. 2 and 4 one can see observed changes in wind speed positively contribute to the synergistic interactions between UHIs and HWs in both daytime and nighttime, as illustrated by the arrows in Fig. 4.

4. Conclusions and discussions

In this paper, the interaction between urban heat islands and heat waves in the lower atmosphere (from the ground to about 100 m above the ground) is studied. Observed vertical profiles of air temperature and wind speed measured at an urban and a rural site in the Beijing metropolitan area are first compared. Results show

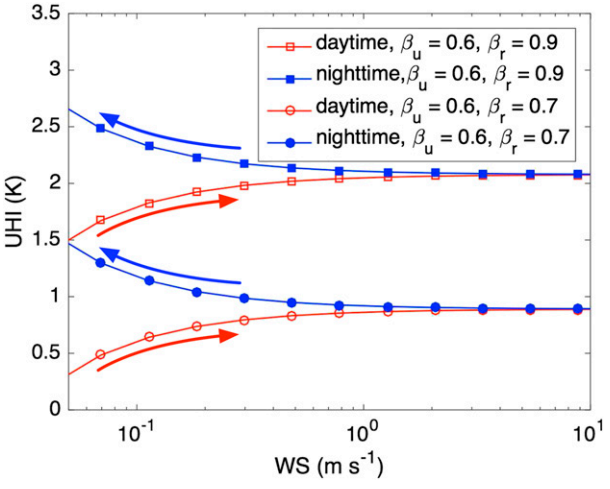

FIG. 4. The simulated UHI effect at 10 m averaged over the urban domain (i.e., between 0 and x_u, which is chosen to be 10 km) as a function of WS ($\mathrm{m\,s^{-1}}$) by the analytical model [Eq. (1)] during daytime ($\Delta Q = -20\,\mathrm{W\,m^{-2}}$) and nighttime ($\Delta Q = 20\,\mathrm{W\,m^{-2}}$). The T_{rs}^* is chosen to be 6.4 K to represent typical urban–rural settings as in the study of LBZ13. The arrows show how changes in the WS contribute to the enhancement of UHI effect during daytime and nighttime.

that the positive interaction between UHIs and HWs, as identified in the studies of LBZ13 and L15 at the surface level, persists across a range of vertical levels (below ~70 m). Interestingly, changes in the urban wind speed under HWs, as compared with the rural wind speed, show opposite signs in daytime and nighttime: during daytime, the urban wind speed is enhanced; during nighttime, the urban wind speed is reduced. The analytical model in LBZ13 is further employed to understand the impact of these changes in the wind speed on the UHI effect. It turns out that the sensitivity of UHI to wind speed strongly depends on the available energy difference: during daytime, the urban–rural available energy difference is negative and the UHI is enhanced when the wind speed increases because of a stronger sensible heating effect; during nighttime, the urban–rural available energy difference is positive and the UHI is reduced when the wind speed increases because of a stronger advective cooling effect. As a result, changes in the wind speed due to HWs positively contribute to the UHI effect during both daytime and nighttime.

The study of L15 identified that urban and rural surface energy budgets responded differently to HWs, which explained the positive interaction between UHIs and HWs at the surface and near the surface. Qualitatively it is shown here that changes in the wind speed also positively contribute to this interaction across a range of vertical levels in the lower atmosphere. However, to what extent these changes in the wind profile explain the vertical profile of this interaction shown in Fig. 1 remains an open question, which is likely a result of the combined impact of changes in the surface energy balance and wind profile. The analytical model provides a good framework to disentangle these contributions. However, the current analytical model is based on a few strong assumptions, such as steady state. Further improvements of the model or numerical simulations are needed to quantify these contributions.

There are other implications of this study. First of all, the observational analysis here is restricted to the Beijing metropolitan area and the summers of 2009 and 2010. It is fairly difficult to pair two sites that have mean meteorological variable measurements at different vertical levels and turbulence measurements. More observational and numerical studies performed over regions of different climates are needed to confirm the results of Beijing. Second, uncertainties in our results remain significant, which is partly due to the limited data coverage. The consistency between observational data and the analytical model results is certainly encouraging and helpful for elucidating the physical mechanisms; nonetheless, using longer data records in the future is recommended for thorough analysis. Last but not least, this study is solely focused on air temperature, while humidity plays an equally important role for many practical applications such as estimation of heat stress. Studies investigating changes in the humidity under HWs are under way.

Acknowledgments. Author TS acknowledges support from the National Natural Science Foundation of China (NSFC) under Grants 51190092 and 51409147 and China Postdoctoral Science Foundation under Grant 2015T80093. Authors LW and ZG acknowledge support from the NSFC under Grants 41405018 and 41275022.

REFERENCES

Anderson, B. G., and M. L. Bell, 2009: Weather-related mortality: How heat, cold, and heat waves affect mortality in the United States. *Epidemiology*, **20**, 205–213, doi:10.1097/EDE.0b013e318190ee08.

——, and ——, 2011: Heat waves in the United States: Mortality risk during heat waves and effect modification by heat wave characteristics in 43 U.S. communities. *Environ. Health Perspect.*, **119**, 210–218, doi:10.1289/ehp.1002313.

Arnfield, A. J., 2003: Two decades of urban climate research: A review of turbulence, exchanges of energy and water, and the urban heat island. *Int. J. Climatol.*, **23**, 1–26, doi:10.1002/joc.859.

D'Ippoliti, D., and Coauthors, 2010: The impact of heat waves on mortality in 9 European cities: Results from the EuroHEAT project. *Environ. Health*, **9**, 1–9, doi:10.1186/1476-069X-9-37.

Garratt, J. R., 1990: The internal boundary-layer—A review. *Bound.-Layer Meteor.*, **50**, 171–203, doi:10.1007/BF00120524.

Grimmond, S., 2007: Urbanization and global environmental change: Local effects of urban warming. *Geogr. J.*, **173**, 83–88, doi:10.1111/j.1475-4959.2007.232_3.x.

IPCC, 2013: *Climate Change 2013: The Physical Science Basis*. Cambridge University Press, 1535 pp., doi:10.1017/CBO9781107415324.

Kovats, R. S., and S. Hajat, 2008: Heat stress and public health: A critical review. *Annu. Rev. Public Health*, **29**, 41, doi:10.1146/annurev.publhealth.29.020907.090843.

Lau, N.-C., and M. J. Nath, 2012: A model study of heat waves over North America: Meteorological aspects and projections for the twenty-first century. *J. Climate*, **25**, 4761–4784, doi:10.1175/JCLI-D-11-00575.1.

——, and ——, 2014: Model simulation and projection of European heat waves in present-day and future climates. *J. Climate*, **27**, 3713–3730, doi:10.1175/JCLI-D-13-00284.1.

Li, D., and E. Bou-Zeid, 2011: Coherent structures and the dissimilarity of turbulent transport of momentum and scalars in the unstable atmospheric surface layer. *Bound.-Layer Meteor.*, **140**, 243–262, doi:10.1007/s10546-011-9613-5.

——, and ——, 2013: Synergistic interactions between urban heat islands and heat waves: The impact in cities is larger than the sum of its parts. *J. Appl. Meteor. Climatol.*, **52**, 2051–2064, doi:10.1175/JAMC-D-13-02.1.

——, and ——, 2014: Quality and sensitivity of high-resolution numerical simulation of urban heat islands. *Environ. Res. Lett.*, **9**, 055001, doi:10.1088/1748-9326/9/5/055001.

——, ——, and H. A. R. De Bruin, 2012: Monin–Obukhov similarity functions for the structure parameters of temperature

and humidity. *Bound.-Layer Meteor.*, **145**, 45–67, doi:10.1007/s10546-011-9660-y.

——, ——, and M. Oppenheimer, 2014: The effectiveness of cool and green roofs as urban heat island mitigation strategies. *Environ. Res. Lett.*, **9**, 055002, doi:10.1088/1748-9326/9/5/055002.

——, T. Sun, M. Liu, L. Yang, L. Wang, and Z. Gao, 2015: Contrasting responses of urban and rural surface energy budgets to heat waves explain synergies between urban heat islands and heat waves. *Environ. Res. Lett.*, **10**, 054009, doi:10.1088/1748-9326/10/5/054009.

Meehl, G. A., and C. Tebaldi, 2004: More intense, more frequent, and longer lasting heat waves in the 21st century. *Science*, **305**, 994–997, doi:10.1126/science.1098704.

Miao, S., J. Dou, F. Chen, J. Li, and A. Li, 2012: Analysis of observations on the urban surface energy balance in Beijing. *Sci. China Earth Sci.*, **55**, 1881–1890, doi:10.1007/s11430-012-4411-6.

Mishra, V., A. R. Ganguly, B. Nijssen, and D. P. Lettenmaier, 2015: Changes in observed climate extremes in global urban areas. *Environ. Res. Lett.*, **10**, 024005, doi:10.1088/1748-9326/10/2/024005.

Oke, T. R., 1982: The energetic basis of the urban heat island. *Quart. J. Roy. Meteor. Soc.*, **108**, 1–24, doi:10.1002/qj.49710845502.

Peterson, T. C., and Coauthors, 2013: Monitoring and understanding changes in heat waves, cold waves, floods, and droughts in the United States: State of knowledge. *Bull. Amer. Meteor. Soc.*, **94**, 821–834, doi:10.1175/BAMS-D-12-00066.1.

Petkova, E. P., H. Morita, and P. L. Kinney, 2014: Health impacts of heat in a changing climate: How can emerging science inform urban adaptation planning? *Curr. Epidemiol. Rep.*, **1**, 67–74, doi:10.1007/s40471-014-0009-1.

Robinson, P. J., 2001: On the definition of a heat wave. *J. Appl. Meteor.*, **40**, 762–775, doi:10.1175/1520-0450(2001)040<0762:OTDOAH>2.0.CO;2.

Smith, T. T., B. F. Zaitchik, and J. M. Gohlke, 2013: Heat waves in the United States: Definitions, patterns and trends. *Climatic Change*, **118**, 811–825, doi:10.1007/s10584-012-0659-2.

Wang, L., D. Li, Z. Gao, T. Sun, X. Guo, and E. Bou-Zeid, 2014: Turbulent transport of momentum and scalars above an urban canopy. *Bound.-Layer Meteor.*, **150**, 485–511, doi:10.1007/s10546-013-9877-z.

——, Z. Gao, S. Miao, X. Guo, T. Sun, M. Liu, and D. Li, 2015: Contrasting characteristics of the surface energy balance between the urban and rural areas of Beijing. *Adv. Atmos. Sci.*, **32**, 505–514, doi:10.1007/s00376-014-3222-4.

Yeh, G.-T., and W. Brutsaert, 1971a: A solution for simultaneous turbulent heat and vapor transfer between a water surface and the atmosphere. *Bound.-Layer Meteor.*, **2**, 64–82, doi:10.1007/BF00718089.

——, and ——, 1971b: A numerical solution of the two dimensional steady-state turbulent transfer equation. *Mon. Wea. Rev.*, **99**, 494–500, doi:10.1175/1520-0493(1971)099<0494:ANSOTT>2.3.CO;2.

Yu, M., Y. Liu, Y. Dai, and A. Yang, 2013: Impact of urbanization on boundary layer structure in Beijing. *Climatic Change*, **120**, 123–136, doi:10.1007/s10584-013-0788-2.